

## Rock slides, rock avalanches and deep seated gravitational slope deformation at the orogeny scale: the case of European

GIOVANNI, Crosta<sup>1\*</sup>

<sup>1</sup>Dept. Earth and Environmental Sciences, UNiv. Milano Bicocca

An orogen scale inventory of large landslides (mainly rockslides), rock avalanches and deep seated gravitational slope deformations (DSGSD) in the European Alps has been prepared by the authors (Crosta et al., 2013, 2014) and results of the analysis are presented in this contribution. The inventory includes: over 2000 large landslides, ranging in area between 0.1 and 17 km<sup>2</sup>, about 300 rock avalanches, ranging between 0.09 and 15.5 km<sup>2</sup>, and a total of 1033 DSGSDs, ranging in size between 0.03 and 108 km<sup>2</sup>. The inventory covers an area of about 110,000 km<sup>2</sup> extending over the alpine territories of Italy, France, Switzerland, Austria and Slovenia, and was prepared by using available satellite imagery (multitemporal, Google Earth, Google, Inc.) and topographic data at different resolutions (DEMs from 1 m x 1m up to 20 m x 20 m for different areas). The inventory was validated against local and regional landslide inventories already available at different scales. Geometrical features and geomorphological parameters have been collected and related to the different phenomena and local settings in order to assess the control of local slope morphology on the occurrence and the geometry of these large instabilities. The frequency/area relationship for the different classes of mapped features is presented. The inventory shows that large landslides are widespread in the Alps with clustering in some sectors of the orogen. Their spatial distribution has been analysed through bivariate and multivariate analysis (mainly Principal Component Analysis and Discriminant Analysis) against a variety of factors, including: lithology, proximity to tectonic structures, seismicity, uplift and exhumation rates, position within the mountain belt and along main and tributary valleys, slope morphometry (e.g. relief, elevation, gradient), ice thickness of glaciers during LGM, and mean annual rainfall. The analysis allowed a preliminary assessment of conditions favourable to the onset and development of large landslides and DSGSD. The occurrence of foliated metamorphic rocks, LGM ice thickness, local relief (and related parameters), slope size, drainage density and river stream power are the local parameters most positively correlated to DSGSD occurrence. Finally, a comparison between the distributions of different phenomena is presented and discussed.

Keywords: landslides, deep seated gravitational slope deformation, rock avalanche, inventory, orogen, European Alps

## Shallow Landslide Susceptibility Mapping Using High-resolution Topography for Areas Devastated by Super Typhoon Haiyan

RABONZA, Maricar<sup>1\*</sup> ; FELIX, Raquel<sup>1</sup> ; LAGMAY, Alfredo mahar francisco<sup>2</sup> ; ECO, Rodrigo narod<sup>2</sup> ;  
ORTIZ, Iris jill<sup>1</sup> ; AQUINO, Dakila<sup>2</sup>

<sup>1</sup>University of the Philippines Diliman, <sup>2</sup>Nationwide Operational Assessment of Hazards

Super Typhoon Haiyan, considered as one of the most powerful storms recorded in 2013, devastated the central Philippines region on 8 November 2013 with damage amounting to more than USD 2 billion. Hardest hit are the provinces of Leyte and Samar. Rehabilitation of the areas that were devastated requires detailed hazard maps as a basis for well-planned reconstruction. Along with severe wind, storm surge, and flood hazard maps, detailed landslide susceptibility maps for the cities and municipalities of Leyte (7,246.7 sq. km) and Samar (13,121 sq. km) provinces are necessary. In order to rapidly assess and delineate areas susceptible to rainfall-induced shallow landslides, Stability INdex MAPping (SINMAP) software was used over a 5-meter Interferometric Synthetic Aperture Radar (IFSAR)-derived digital terrain model (DTM) grid. Topographic, soil-strength and hydrologic parameters were used for each pixel of a given DTM grid to compute for the corresponding factor of safety. The landslide maps generated using SINMAP are highly consistent with the landslide inventory derived from high-resolution satellite imagery from 2003 to 2013. The methodology addresses the need for rapidly generated shallow landslide susceptibility maps and detailed landslide susceptibility classification which is useful to identify safe and unsafe areas for reconstruction and rehabilitation efforts. These shallow landslide susceptibility maps have been made freely available to different relief and rehabilitation agencies in Typhoon Haiyan ravaged areas. These maps complement the debris flow and structurally-controlled landslide hazard maps that are also being prepared for rebuilding Haiyan's devastated areas.

Keywords: Landslide, Natural Hazard, SINMAP, Susceptibility Map, Spatial Analyses, Philippines

## Triggering mechanism of shallow landslides in Izu-Ohshima Island, Japan.

IMAIZUMI, Fumitoshi<sup>1\*</sup> ; MIYAMOTO, Kuniaki<sup>2</sup> ; ISHIKAWA, Yukina<sup>3</sup>

<sup>1</sup>Graduate School of Agriculture, Shizuoka University, <sup>2</sup>Faculty of Life and Environmental Sciences, University of Tsukuba,

<sup>3</sup>Faculty of Agriculture, Shizuoka University

On October 16, 2013, Typhoon Wipha attached west slope of the Mt. Mihara in Izu-Oshima Island, Japan, and induced shallow landslides with large areas. These landslides killed 36 people, and 3 people are still missing. Sliding surfaces of these landslides were located at the boundary between high permeable scoria (and tephra) layer and low permeable loess layer. Aerial photograph investigation in the period from 1945 to 2013 showed that only one rainfall event, Typhoon Ida in 1958, induced many landslides in the area before the Typhoon Wipha. Depth of the sliding surfaces during this Typhoon was similar to that during Typhoon Wipha. We derived spatial distribution of the pore water pressure in the two-dimensional slopes with multi-layer structures on the basis of the continuity equation and equation of motion for seepage flow. Our analyses elucidated that the pore water pressure does not agree with hydrostatic pressure if the lower end of the saturated zone is not locating on the impermeable layer. Our simulation of the seepage flow during the Typhoon Wipha and Typhoon Ida showed that the pore water pressure was highest at the boundary between tephra and loess layers on which sliding surfaces of the landslides were located. Pore water pressure during other large rainfall events without landslide was below that during Typhoon Wipha and Ida. Consequently, increasing in the pore water pressure at the boundary between tephra and loess is the important factor triggering landslides in the Izu-Oshima Island.

Keywords: landslide, pore water pressure, Izu-Oshima, multi-layer soil structure

## Flowsliding in volcanic ash slope during heavy rainfall: A Case Study of 2013 Izu Oshima Landslides

WANG, Gonghui<sup>1\*</sup> ; JIANG, Yao<sup>2</sup>

<sup>1</sup>Disaster Prevention Research Institute, Kyoto University, <sup>2</sup>Graduate School of Science, Kyoto University

On Oct. 16, 2013, catastrophic shallow landslides were triggered on a wide area of the west-side hill slopes in Izu-Oshima Island, Japan, by the heavy rainfall accompanying Typhoon No.26 (Wipha). The displaced landslide material traveled long distance with rapid movement, resulting in 35 dead, 4 missing, and 46 buildings being completely destroyed on the downstream area of Motomachi area. To understand the initiation and movement mechanisms of these shallow landslides, we took sample from the source areas and examined their shear behavior under partially drained or undrained condition. We performed flume tests to trigger landslides by rainfall, and examined the variation of soil moisture, pore-water pressure and landslide movement. Test results showed that high pore-water pressure could be built up and maintained within the displaced landslide material, resulting in rapid flowsliding movement, irrespective of the nature of very shallow sliding mass. Results obtained from the simulation of landsliding shows that the high mobility resulted from liquefaction failure of displaced landslide materials. Field observation also revealed that wind load to the trees on steep slopes might have played key role on the triggering of the slope failure on wide areas.

Keywords: Flowslide, heavy rainfall, volcanic ash slope, wind load, trees

## An Improved Method for Classifying Debris Flow Disaster Potential

WU, Tingyeh<sup>1\*</sup>

<sup>1</sup>NATIONAL SCIENCE AND TECHNOLOGY FOR DISASTER REDUCTION, TAIWAN

This study aims to clarifying torrents with debris flow disaster potential. A special debris flow occurred at Hualien County during typhoon Saola in 2012. A turning curve occurred and community which was not supposed to be under disaster potential damaged by debris flow. The previous study shows the main reasons of this event are continuous rainfall event, specific geological material and topographic conditions. The disaster represents the insufficiency of the current method to classify the debris flow potential. Therefore, this study follows the findings and intends to confirm if the similar torrents exist or not. The study cases were selected from the torrents with debris flow potential defined by the authority and 5 torrents were determined by their geological condition with metamorphic rock material. The debris flow simulations were carried out by Flo-2D numerical model with three continuous designed rainfall events. The simulation results show that turning curve occurred at some of the cases, but some did not. Authors analyzed their topographic conditions to check the differences of the simulation result. From the gradient of the flowing part and the topographic conditions of alluvial fan, the criteria of the debris flow resulting in turning curve could therefore be summarized, which could be the indexes to clarify the probable torrents with debris flow potential.

Keywords: Flo-2D, debris flow disaster potential, turning curve, topographic criteria, second debris flow disaster

## Karangkobar landslide, Banjarnegara district central of Java Province Indonesia

DASA TRIANA, Yunara<sup>1</sup> ; KRISTIANTO, Kristianto<sup>1\*</sup> ; NURSALIM, Asep<sup>1</sup>

<sup>1</sup>Geological Agency, Ministry of Energy and Mineral Resources of Indonesia

In Indonesia has been 436 landslides during 2014 period. 115 of them occurred in the Central of Java Province. One of the landslide that evolve in to debris flow and cause great casualties and damages, have occurred on December 12nd, 2014 in Jemblung, Sampang Village, Karangkobar, Banjarnegara Regency. Geographically it is located at 109°43'15.3912" E and 7°16'52.5828" S. This landslide causing more than 100 people died and property losses. Regionally disaster location composed by Jembangan volcanic rocks consisting of andesitic lava and volcanic rocks clastic.

The types of landslides is rotational sliding and the types of materials are debris. This landslide triggered by heavy rainfall. Climatological Agency of Banjarnegara data showed that rainfall accumulation reached 349 mm in eleven days before landslide, while at the time of the incident was recorded 101.8 mm.

This even is interesting because of the material dispersion mechanism happens to be a large of the distribution. Distance of debris flow up to large area and has caused damage along its flow track. Distribution of debris controlled by the viscosity of the material and topography.

Keywords: Jemblung, debris, rainfall, Banjarnegara, topography

## Estimation of dynamic friction of the Akatani landslide based on the waveform inversion and numerical simulation

YAMADA, Masumi<sup>1\*</sup> ; MATSUSHI, Yuki<sup>1</sup> ; MANGENEY, Anne<sup>2</sup>

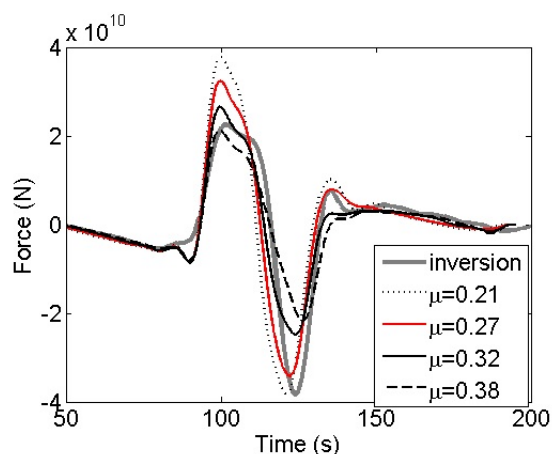
<sup>1</sup>DPRI Kyoto University, <sup>2</sup>IPGP

We performed numerical simulations of the 2011 deep-seated Akatani landslide in central Japan to understand the dynamic friction process of the landslide. By comparing the forces obtained from the numerical simulation and seismic waveform inversion, the most probable friction model was estimated.

Based on the numerical simulation, dynamic coefficient of friction was well constrained as 0.3 and a rapid increase of the velocity and the associated drop of the coefficient of friction were observed right after the onset of sliding.

The friction law that controls landslide dynamics is velocity-weakening with sudden drop after the initiation of sliding, which accelerates the deep-seated landslide. The friction model calibrated here using seismic data helps to understand the dynamics of the landslide and provide the basic property of the shearing resistance of the slip plane.

Keywords: deep-seated landslide, dynamic friction, seismic waveform, numerical simulation, granular material



## Seismic observation in a large, incipient rockslide on an anaclinal slope

DOI, Issei<sup>1\*</sup> ; WANG, Gonghui<sup>1</sup> ; KAMAI, Toshitaka<sup>1</sup> ; CHIGIRA, Masahiro<sup>1</sup>

<sup>1</sup>Disaster Prevention Research Institute, Kyoto University

Japan has experienced mega earthquakes and catastrophic coseismic landslides (e.g. the 2004 Niigata Chuetsu earthquake and the 2011 off the Pacific coast of Tohoku Earthquake). However, it is not well understood how the slopes behave under strong shaking because seismic observations on the slope are crucially insufficient.

In 2014, we started seismic observations in Kawashimo landslide, a large, incipient rockslide on an anaclinal (in-facing) slope in Ehime Prefecture, southwest Japan. The length, the relative height and the width of the Kawashimo landslide are approximately 700 m, 450 m and 150 m, respectively. On the lower side of the landslide, rocks are highly fractured so that long cracks are densely observed. We installed two seismometers there, with the separation distance of 30 m. Ten earthquakes with high signal to noise (S/N) ratios were recorded from Oct. 30, 2014 to Jan. 7, 2015. We first calculated the spectra using the waveforms of ten seconds after the twice of S times because scattering waves are considered to be coming from all the directions in this time window. Then, we took the spectral ratios of two horizontal components to the vertical one for the purpose of cancellation of source spectra. The obtained spectral ratios are stable among ten earthquakes we analyzed, regardless of their back-azimuths. Horizontal components have a spectral peak around 7 Hz at both stations but the peak values of the spectral ratios are larger in NS components than in EW at one station, indicating that dip direction of the slope and/or shape of the landslide block may affect the characteristics of slope vibration. These results will provide basic information for considering the motion of the landslide materials on a slope during earthquakes.



## Acoustic emissions preceding the stress drops in locally sheared granular materials

JIANG, Yao<sup>1\*</sup> ; WANG, Gonghui<sup>2</sup> ; KAMAI, Toshitaka<sup>2</sup>

<sup>1</sup>Graduate School of Science, Kyoto University, <sup>2</sup>Disaster Prevention Research Institute, Kyoto University

For better understanding the mechanisms of rapid landsliding events, both the initial and long runout motion in which granular masses flow with extremely low friction is essential. Many studies had been performed to understand such kind of the unusual physical feature. However, the progressive maturation of these catastrophic landslides is still lack of enough scientific evidence. Importantly, acoustic emission (AE) technique provides the opportunity to study the grain-scale shear deformation of granular assemblies, and can be used to directly investigate the physical processes and failure mechanisms. Herewith, we employed a high frequency range of AE sensor to capture the elastic waves due to the abrupt perturbations of internal forces and release of strain energy, and the dependence of particle size and shear velocity on the AE characteristics has also been examined. We found that the dynamical drops of shear resistance and the amplitude of AE waveforms were larger with increase of the particle size. We also analyzed the relationship between AE rates (per second) and shear velocity, which indicated that the AE rates would increase with increase of the shear velocity. Ultimately, we examined the frequency contents and occurrence time of AE waveforms, and we found that the ultrasonic precursors occurred prior to the dynamic failures among granular materials.

Keywords: acoustic emission, stress drop, granular materials, particle size, shear velocity, rapid landslides

## Debris avalanches of pyroclastic fall deposits induced by the 1949 Imaichi earthquake

CHIGIRA, Masahiro<sup>1\*</sup> ; SUZUKI, Takehiko<sup>2</sup> ; WANG, Gonghui<sup>1</sup> ; TOBITA, Tetsuo<sup>1</sup>

<sup>1</sup>Disaster Prevention Research Institute, Kyoto University, <sup>2</sup>Tokyo Metropolitan University

Debris avalanches of pyroclastic fall deposits have been frequently induced by earthquakes in circum pacific countries, causing severe damage. Recent earthquakes that induced that type of landslides are 2011 Tohoku earthquake, 1984 Naganoken Seibu earthquake, 1978 Izu-Oshima-Kinkai earthquake, 1969 Tokachi-Oki earthquake, and 1949 Imaichi earthquake, in which landslides induced by the 1949 Imaichi have much less record than the others. Landslides induced by the 1949 Imaichi earthquake with a magnitude of 6.4 has been reported to have induced numerous numbers of landslides by Morimoto (1951) but their distribution has not been well plotted on a map and the slid materials are not well specified. We surveyed the affected area using high-resolution DEMs obtained by the airborne LiDAR and made field surveys. Comparison between the high-resolution DEMs and local landslide distribution maps showed that there are two types of landslide, one is a deep landslide with a sliding surface along the Kanuma Pumice Fall Deposot in a depth of 5-6 m and the other is a shallow landslide with a sliding surface probably along the base of the Imaichi Pumice Fall Deposit in a depth of 2-3 m. The deep landslides are rather easy to identify using high-resolution DEMs, and in addition to the 1949 landslides, we identified older deep landslides, which are assumed to have sliding surfaces in the same horizon with the 1949 landslides. Topographic features of shallow landslides may be erased fast, so we suppose older landslides cannot be identified on high-resolution DEM images.

Keywords: earthquake, landslide, tephra, pumice

## Rapid Weathering and Salt Water Migration Processes near a Slope Surface in Plio-Pleistocene Mudstone Areas in Taiwan

HIGUCHI, Kohei<sup>1\*</sup> ; CHIGIRA, Masahiro<sup>2</sup> ; LEE, Der-her<sup>3</sup> ; WU, Jian-hong<sup>3</sup>

<sup>1</sup>Grad. Sch. of Front. Sci., Univ. Tokyo, <sup>2</sup>DPRI, Kyoto Univ., <sup>3</sup>Dept. of CE, Natl. Cheng Kung Univ.

Badlands consisting of barren slope surfaces, sharp ridges, and v-shaped gullies are widely formed in Plio-Pleistocene mudstone in southwest Taiwan due to rapid weathering and erosion near the slope surface. The mudstone, which formed in the syn-collisional Plio-Pleistocene foreland sequence, has high density with a void ratio as low as 0.2 and has pore water chemistry similar to the seawater. In this area under the humid, subtropical climate with distinct dry and rainy seasons, since the mudstone slope surfaces are eroded as high as 9 cm/y in average in the rainy season, paved roads such as national express way are frequently damaged by slope failure hazards. To understand the mechanism of rapid erosion, we monitored water content and salinity near the slope surface and found that salt water migrates from the depth to the surface during the dry season, and salt precipitated on crack surfaces. After the dry season, rainfalls in the early rainy season dilutes the salinity, and closes desiccation cracks, consequently slowing the downward migration of water near the slope surface. The wetting of dry rocks and dilution of pore water near the slope surfaces deteriorates the rock and disperses rock-forming grains. The deteriorated surfaces are eroded during subsequent rain in the late rainy season. After the erosion, migration of salt water from the depths to the surfaces occurs again during the subsequent dry season.

Keywords: Plio-Pleistocene Mudstone, Rapid Weathering, Badlands, Monitoring, Salt Water Migration